



## WIDEBAND AND DUAL-BAND ANTENNAS WITH BAND-NOTCHED USING ELECTROMAGNETIC BAND-GAP STRUCTURE

I. Nasidi<sup>1,\*</sup> and H. Bello<sup>2</sup>

<sup>1</sup>Department of Electrical and Electronics Engineering, Usmanu DanFodiyo University, Sokoto, Nigeria.

<sup>2</sup>Department of Information and Communication Technology, Usmanu DanFodiyo University, Sokoto, Nigeria.

\*corresponding author (Phone Number: +234-806-549-8184. Email: [ibronasidi@yahoo.com](mailto:ibronasidi@yahoo.com))

Article history: Received 02 October, 2021. Revised 24 October, 2022. Accepted 26 October, 2022

### Abstract

*This paper presents a single-element microstrip spade-shaped patch antennas with a partial ground plane, integrated with an electromagnetic band-gap (EBG) structure, and fed with a microstrip feedline to achieve wide-band, dual-band and band-notched characteristic. Two similar mushroom-like EBG structures built into the wide-band antenna were used to suppress a specific band, resulting in dual-band. The wide-band antenna achieved a broad bandwidth of 9GHz from 5-14GHz, with a maximum gain of 6.8dBi. Based on the simulation and measured results, the wide-band antenna offers 89% fractional bandwidth for a voltage standing wave ratio less than 2 (VSWR < 2). The EBG provides a band-notch with a bandwidth 3GHz from 8-11GHz, leaving dual-band with bandwidths of 2GHz and 1.5GHz centred at 7GHz and 11GHz, respectively. Surface current distribution and parametric studies were conducted to better understand the behaviour and influence of the EBG parameters. The simulation results were validated through experimental measurement, and both agreed well. The antennas could be used for 5G wireless communication and filtering.*

**Keywords:** Antenna Design, Band-notch, Dual-band, Electromagnetic Band-gap, Wideband.

### 1.0 INTRODUCTION

Microstrip patch antenna has attracted immense attention in wireless communication research due to their advantages, which include low profile, low cost, ease of fabrication and integration in circuits. However, the microstrip patch antenna suffers from narrow bandwidth and low gain [1]. Recently, microstrip patch antenna research interests have shifted towards operation at high frequencies such as millimeter-wave spectrum [2], [3], due to limited spectrum at a low frequency and potential possibilities offered by high frequency such as high gain and increased bandwidth. In 5G wireless communication applications, a high frequency spectrum above 6GHz is being utilized. 5G offers many advantages such as multiple connected devices, low latency, improved reliability, and a very high data rate [4]. For a high data rate transmission and reception, an antenna that supports wide bandwidth operation is required. The approaches to enhance the bandwidth of a microstrip patch antenna are classified into three. Firstly, by

lowering the Quality factor (Q-factor). The patch of a microstrip antenna can be rectangular, square, circular or elliptical. So, by changing the patch configuration to another shape such as T-shape [3], or increasing substrate thickness, the Q-factor is lowered. Secondly, by using an impedance matching network [5], [6]. Thirdly, by Introducing multiple resonances [7].

Here, spectrum 6-12GHz is being considered for the antenna operation. However, within this spectrum, there exists another band of 10.68-10.7GHz where the radio regulation (foot note 5.340 in the International Telecommunication Union table of frequency allocation) prohibits radiation [8]. Therefore, a method to notch radiation in this band has to be explored. Traditionally, band-notching has been realized in an antenna by using a resonant element such as slots of various shapes etched on the patch or the ground plane, and using parasitic elements [9]–[14]. The use of slots for band-notching, however, limits the control over the notch bandwidth. To

overcome this limitation, an electromagnetic band gap (EBG) structure is been employed [13]. Several designs that combine an antenna with EBG for a specific application have previously been reported. For instance, Ayopet al. [15], reported a dual-band EBG structure incorporated into an ultra-wideband antenna to perform dual-band rejection in a double-layer substrate. The use of a double-layer substrate increases the substrate thickness, which leads to the excitation of surface waves, limiting the antenna's performance to a gain of only 0.8567dBi. Similarly, Yazdi and Komjani [16], demonstrated a band-notched ultra-wideband monopole antenna for single-band rejection around 5.5GHz with a rejection bandwidth of 0.7GHz using four EBG structures. The use of four EBG for a single and narrow band rejection is prodigal, over design, and increases the design's complexity. Hirano and Hirose [17], also reported a wideband tapered slot antenna using EBG for low direct coupling studies. The wideband antenna covers 6-12GHz and the EBG offers dual band-reject at 4.98GHz and 13.8GHz. However, the notched bandwidth is very narrow. Moreover, the EBG structure has been used in microstrip antennas for surface wave suppression [18], [19], gain enhancement [20], noise suppression [21], [22], and mutual coupling reduction [23].

In this paper, we present wideband and dual-band antennas with band-notch characteristics. EBG structures were used to notch a specific band in a wideband antenna to produce dual 5G bands. The design was carried out in two phases. In the first phase, a wideband antenna was designed and ultra-wide bandwidth was achieved by combining the resonances of the spade-shaped patch and a partial ground plane. The ultra-wideband covers a bandwidth of 9GHz from 5-14GHz with a voltage standing wave ratio (VSWR) of less than 2 and a maximum gain of 6.8dBi. In the second phase, an EBG structure was integrated into the designed wideband antenna to filter out the undesired band, leaving only the dual 5G bands of interest. The band-notch was realized using two similar mushroom-like square-shaped EBGs. A band-notch with a bandwidth of 3GHz covering 8-11GHz and dual-band with center frequency at 7GHz and 11.45GHz with bandwidths 2GHz and 1.5GHz, respectively, were achieved. When compared to previous reports [17], [24], [25], our results are better in terms of operational bandwidth, notch bandwidth, and gain. The EBG provides the largest band-notch possible without affecting the same radiation pattern of the antenna observed in the far-field region. We

carried out an experimental measurement for the reflection coefficient ( $S_{11}$ ) of the proposed antenna structures. The simulation and experimental results for the reflection coefficient agree well.

## 2.0 MATERIALS AND METHODS

In this work, CST microwave studio software was used for the design and simulation of the antennas. To avoid the excitation of surface waves, a suitable substrate with appropriate dielectric constant and thickness should be chosen for the antenna design. Consequently, an FR4 substrate with a dielectric constant of 4.6 and thickness of 1.6mm was used. To design a rectangular patch, a resonant frequency  $f_r$  of 10GHz is chosen and used to calculate the initial dimensions (width  $w$  and length  $l$ ) of the patch using transmission line model equations (1)-(2) [1]. Secondly, an elliptical strip (whose diameter is  $w$ ) was attached to transform the rectangular patch into a spade-shape. This is purposely done to increase the patch and extend the current distribution around the patch, resulting in a low Q-factor [9]. A microstrip feedline is used to feed the patch, and is required to have low insertion loss and controllable characteristic impedance  $Z_0$ . The microstrip feedline dimensions (width  $w_f$ , length  $l_f$ ) were calculated based on the detail in reference [1]. The microstrip feedline is positioned such that the input impedance is  $50\Omega$ . Figure 1(a) depicts the proposed spade-shaped antenna geometry. The patch and the microstrip feedline were designed on the front side of the substrate. A partial ground plane of resonance frequency at 6.5GHz is designed on the backside of the substrate.

$$w = \frac{c}{2f_r} \sqrt{2/\epsilon_r + 1} \quad (1)$$

$$l = \frac{c}{2f_r \sqrt{\epsilon_r}} \quad (2)$$

Where,  $c$  is the free space speed of light,  $f_r$  is the resonant frequency, and  $\epsilon_r$  is the relative permittivity of the substrate.

In the second phase of the design, the proposed spade-shaped antenna geometry of figure 1(a) is integrated with two similar mushroom-like square-shaped EBGs beside the feedline as shown in figure 1(b). As depicted in figure 1(c), the EBG has four parts: a dielectric substrate, a metal EBG patch, a metal ground plane, and a vertical 'vias' that connects the

EBG patch to the ground plane. Equations (3) - (6) were used to calculate the initial dimensions of the EBG parameters [13].

$$W_e = 0.1\lambda_{9GHz} \quad (3)$$

$$h = 0.04\lambda_{9GHz} \quad (4)$$

$$g = 0.02\lambda_{9GHz} \quad (5)$$

$$r = 0.005\lambda_{9GHz} \quad (6)$$

Where  $\lambda$  is the wavelength at the 9GHz resonant frequency of the EBG,  $W_e$  is the EBG patch width,  $h$  is the substrate thickness,  $r$  is the 'vias' radius, and  $g$  is the gap between the EBG patch and the microstrip feedline. The optimized EBG parameters that give the desired band-notch are:  $W_e = 2.3mm$ ,  $g = 0.7mm$ ,  $h = 1.6mm$ , and  $r = 0.2mm$ .

As shown in figure 1(c), the lumped element model described an EBG structure as a resonant circuit [13]. That is, the gap between the EBG patch and microstrip feedline, which are both metals, is modelled as a capacitance and denoted as  $C_1$ . Similarly, the distance between the EBG patch and the ground plane, both of which are metals, depicts capacitance and is denoted as  $C_2$ . The flow of current from the EBG patch to the ground through the 'vias' modelled an inductance and is denoted as  $L$ . The values for the inductance  $L$ , the capacitance  $C$ , and the resonance frequency  $f_0$  of the circuit were calculated from the EBG parameters using equations (7) – (9) [13]. A narrow band-notch was obtained using a unit EBG structure [26]. To provide a wide band-notch, we propose two EBG structures on opposite sides of the microstrip feedline. The two EBG structures are a method of reducing capacitance by connecting another capacitance in series, resulting in a small equivalent capacitance. A decrease in capacitance results in an increase in resonance frequency for a given value of inductance. Thus, notch bandwidth increases.

$$C = \frac{W_e \epsilon_0 (1 + \epsilon_r)}{\pi} \cosh^{-1} \left( \frac{W_e + g}{g} \right) \quad (7)$$

$$L = \mu_0 h \quad (8)$$

$$f_0 = \frac{1}{2\pi\sqrt{LC}} \quad (9)$$

Where,  $C = C_1 + C_2$  is the equivalent capacitance,  $f_0$  is the resonance frequency;  $\epsilon_r$ ,  $\epsilon_0$ , and  $\mu_0$  are the substrate relative permittivity, free space permittivity, and free space permeability, respectively. Table 1 shows the dimensions of the two proposed antennas. Both antennas have an overall dimension of  $25\text{ mm}^2 \times 20\text{ mm}^2$ , and were fed by a  $50\Omega$  microstrip line with an SMA connector, as shown in figure 1(d).

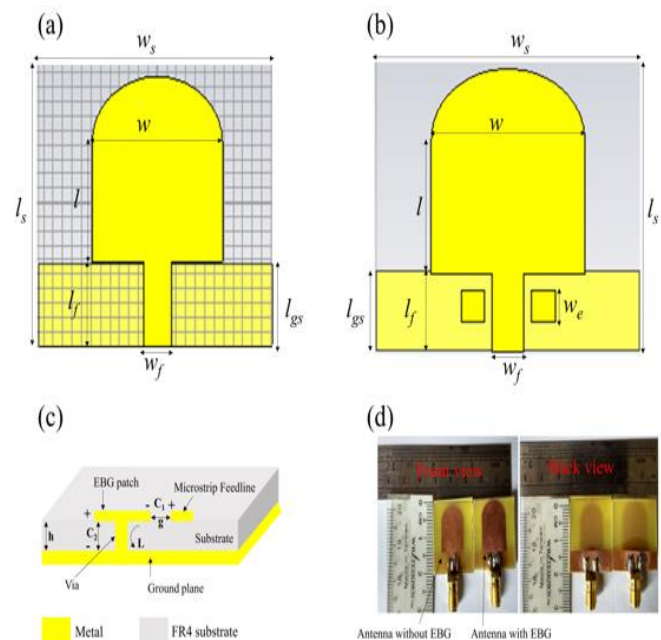


**Figure 1:** Proposed antenna geometries (a) with a spade-shaped patch, microstrip feedline, and a partial ground plane, (b) with two similar square-shaped mushroom-like EBG structures near the feedline, (c) the EBG's lump element  $LC$  model, (d) fabricated antennas on FR4 substrate with an SMA connector.

**Table 1:** Dimensions of the two proposed antennas

| Antenna parameters | $l_s$ (mm) | $W_s$ (mm) | $l$ (mm) | $W$ (mm) | $l_f$ (mm) | $W_f$ (mm) | $l_{gs}$ (mm) | $W_e$ (mm) | $g$ (mm) | $r$ (mm) |
|--------------------|------------|------------|----------|----------|------------|------------|---------------|------------|----------|----------|
| wideband           | 20         | 25         | 8.3      | 13.7     | 6          | 2.98       | 5.7           | -          | -        | -        |
| with EBG           | 20         | 25         | 9.37     | 14.5     | 6          | 2.98       | 4.5           | 2.3        | 0.7      | 0.2      |

### 3.0 RESULT AND DISCUSSION

The simulation results were obtained using CST software, which was further validated with the results

obtained from the experiment which was measured using a network analyser.

### 3.1 RESULTS FOR WIDEBAND ANTENNA

Figure 2(a) depicts the wideband antenna's simulated (dashed line) and measured (solid line)  $S_{11}$ (dB). It can be seen that the simulated and measured results cover frequency ranges of 5-14GHz and 6-14GHz, respectively, with  $S_{11} < -10$ dB. Thus, both results provide an ultra-wide bandwidth of 9GHz, corresponding to an 89% fractional bandwidth. This result is about 2.96 times larger than the result of reference [24], and 1.08 times larger than the result of reference [25]. The ultra-wide bandwidth is achieved by combining the resonances of the spade-shaped patch (designed to resonant at 10GHz), and a partial

ground (designed to resonant at 6.5GHz). Figure 2(b) shows VSWR against frequency. It can be noticed that the antenna has  $VSWR < 2$  over the entire ultra-wide bandwidth. This indicates that the antenna has good impedance matching. Figure 2(c) presents the gain of the antenna. As can be seen, the antenna has a maximum gain of 6.8dBi. Also, except at 8GHz, the gain increases with increasing frequency. This is due to the weak radiation intensity, large beam width, and non-directional pattern at this particular frequency noticed in the radiation pattern (not included here). This gain of the antenna is one order of magnitude better than the gain reported in reference [17].

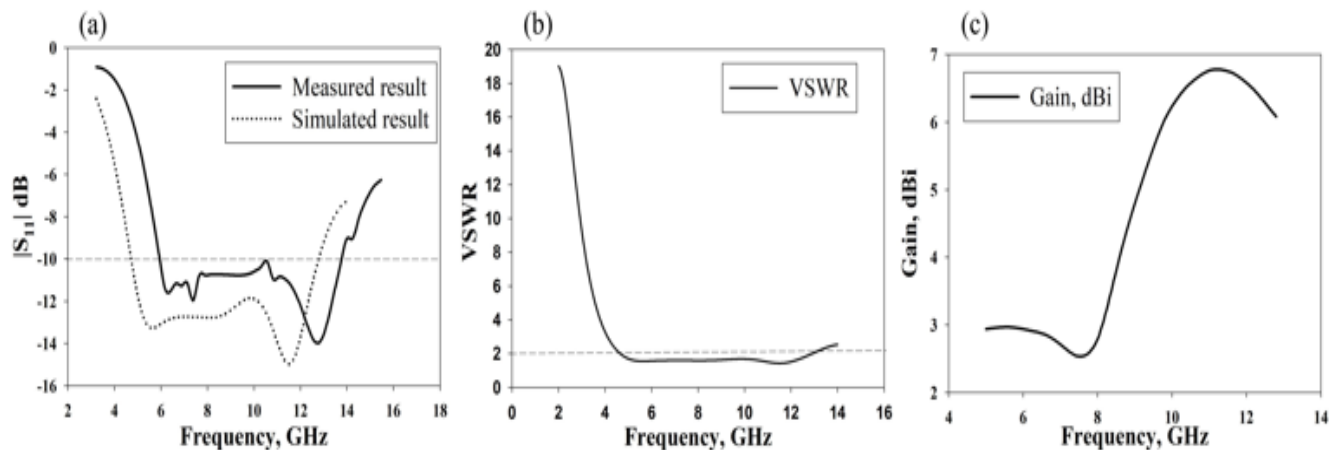


**Figure 2:** Wideband antenna results (a) measured and simulated  $S_{11}$  against frequency, (b)  $VSWR < 2$  over the entire ultra-wide bandwidth, (c) Maximum gain of 6.8dBi.

### 3.2 RESULTS FOR WIDEBAND ANTENNA WITH EBG

The simulation (solid line) and measured (dashed line)  $S_{11}$  (dB) of the wideband antenna with EBG are depicted in figure 3(a). The simulation results show that by integrating EBG into the antenna, the ultra-wideband that was initially obtained has become a dual-band with a band-notch in the middle. The notched band covers 8-11GHz equivalent to a bandwidth of 3GHz with  $S_{11} > -10$ dB. The dual-band have a center frequency at 7GHz and 11.45GHz with bandwidths of 2GHz and 1.5GHz, respectively, for  $S_{11} < -10$ dB. The EBGs achieved a band-notch with a fractional bandwidth of 32% which is higher than the 30.4% reported by Malekpoor et al. [24]. With  $S_{11} > -10$ dB, the measured results show a band-notch bandwidth of 2GHz centered at 10GHz. The measured dual-band are centred at 6.75GHz and 11.35GHz with bandwidths of 4.5GHz and 1.3GHz, respectively, for  $S_{11} < -10$ dB. This shows that the simulation and measured results are in good agreement. Figure 3(b) presents the VSWR of the antenna with EBG. It could

be seen that the value of VSWR at the band-notched range of 8-11GHz is greater than 2, and the VSWR of the dual-band of 6-8GHz and 10.7-12.2GHz is less than 2. This indicates that the EBG offers the required mismatch to create the band-notch. Figure 3(c) illustrates the gain of the antenna with EBG. It could be observed that within the band-notched range of 8-11GHz, there is a sharp decrease in the gain which goes to negative. This negative value of gain indicates that the antenna patch is not radiating in any direction at this band due to the presence of the EBG.

Figure 3(d) depicts the simulation radiation pattern of the two antennas in E-plane, one with EBG (dashed line) and one without the EBG (solid line), at 9GHz, a frequency completely covered by the EBG operation (band-notched frequency). It could be observed that both radiation patterns are identical with a somewhat distorted dumbbell shape. Therefore, it can be deduced that the EBG does not affect the radiation pattern observed at the far-field region. The distortion

in the radiation pattern shape could be due to the excitation of the higher-order mode [27].

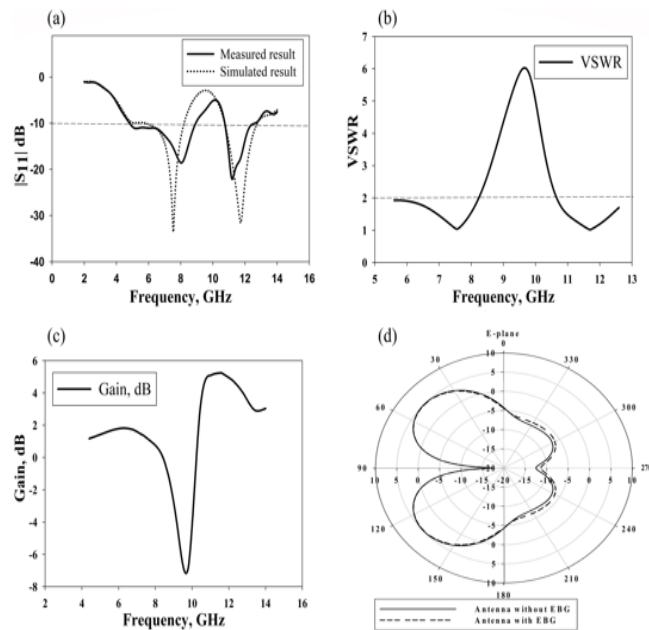


**Figure 3:** Results for the antenna with EBG (a) Simulation and measured  $S_{11}$ (dB), (b)  $VSWR > 2$  in the band-notched range of 8-11GHz and less than 2 elsewhere, (c) Gain: negative gain in the band-notched range of 8-11GHz and positive elsewhere, (d) E-plane radiation pattern exhibiting a dumbbell shape for both antennas at 9GHz.

### 3.3 SURFACE CURRENT DISTRIBUTION

The surface current distribution at 6GHz, 9GHz, and 12GHz are studied to better understand the behavior of the EBG, as shown in figure 4(a)-(c). Figures 4(a) and 4(c) depicts the EBG's operation at 6GHz and 12GHz, respectively. It could be observed that the EBGs are not active because there is a weak current concentration around them. In other words, the injected current is not blocked by the EBG; and thus, reaches the patch and got radiated by the spade-shaped patch and the partial ground plane, as indicated by the strong current concentration around the patch.

Figure 4(b) shows the EBG operation at 9GHz which is an operating frequency completely covered by the EBG bandwidth. It can be seen that the two EBGs are active as depicted by the strong current concentrated around them. This prevents the injected current from reaching the antenna patch. Therefore, it could be deduced that the band-notched characteristic was achieved by the EBG in two ways [28]: firstly, the EBG degrades the impedance matching of the antenna, as depicted by the VSWR curve (figure 3(b)); hence, less energy is radiated to free space. Secondly,

the EBG changes the current distribution of the antenna, as depicted in figure 4(b).

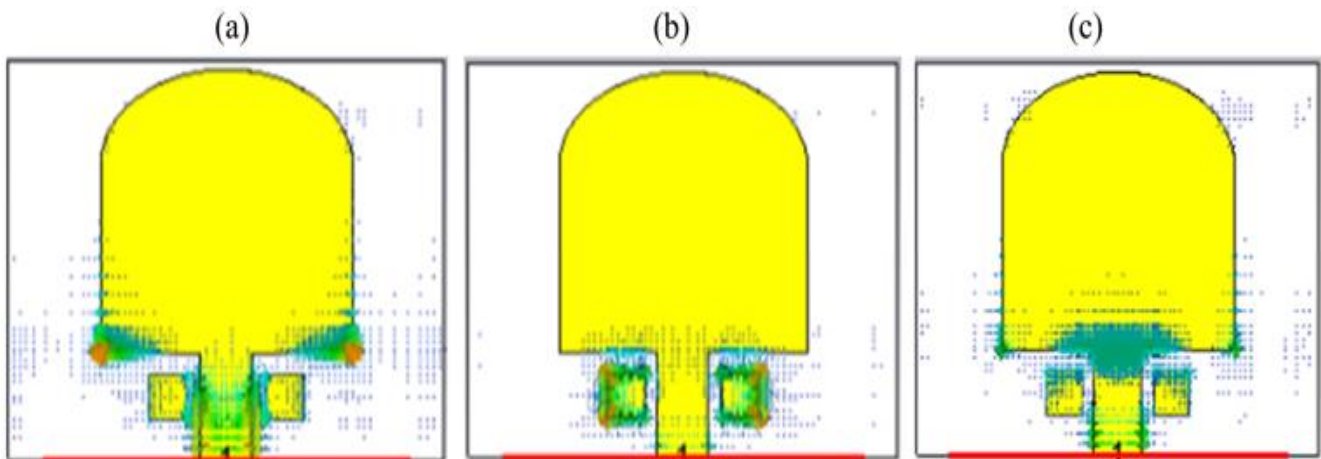
### 3.4 PARAMETRIC STUDY

In this study, a simulation-based manual parameter sweep is carried out on the CST software to determine how the band-notch changes when the EBG parameters change. The parameters affecting the EBG performance are: the EBG patch width ' $W_e$ ', the gap ' $g$ ' between the feedline and EBG, and the ' $vias$ ' offset. When studying the effect of one parameter, other parameters remain unchanged. The VSWR, which is a function of the reflection coefficient ( $S_{11}$ ), is used to characterize the effect of the parameter sweep.

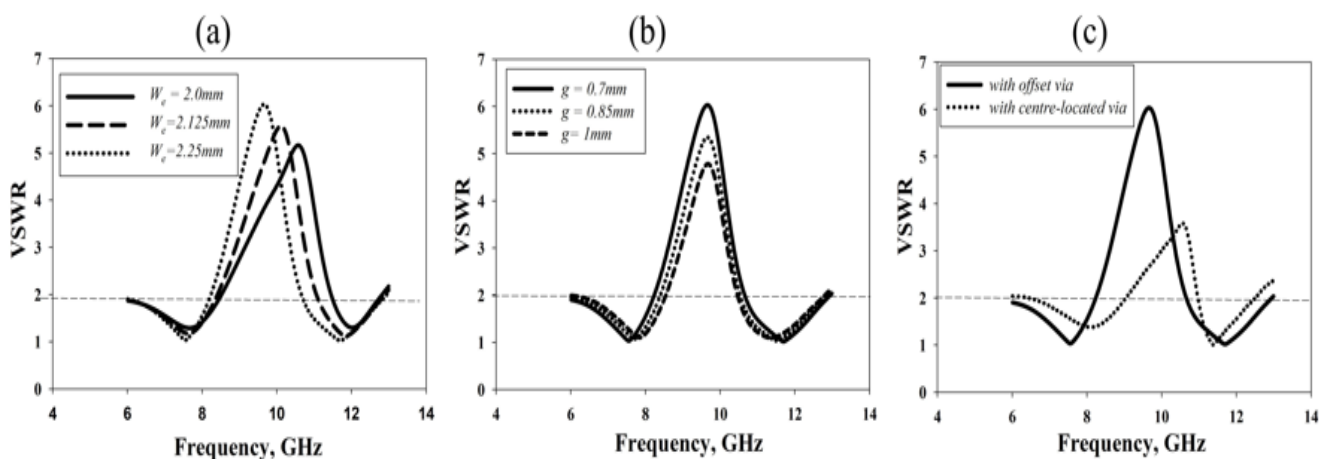
Figure 5(a) shows the VSWR variation with different EBG patch width ' $W_e$ ' values. The EBG patch width ' $W_e$ ' is varied from 2.0mm (solid line), 2.125mm (dashed line), and 2.25mm (dotted line). As the ' $W_e$ ' increases, the band-notch shifts to a lower frequency thereby decreasing the notched bandwidth. Moreover, the curve shape becomes steeper which increases coupling. This physics could be explained as follows: increasing the ' $W_e$ ' is equivalent to increasing the metallic area which is directly proportional to increasing the capacitance (5). Therefore, increasing capacitance results in a decrease in resonant frequency and consequently a decrease in notched bandwidth (7).

Figure 5(b) depicts the change in VSWR as the gap width ' $g$ ' changes. The ' $g$ ' value was increased from 0.7mm (solid line), 0.85mm (dotted line) to 1mm (dashed line). It could be noticed that as the gap increase, the notched band narrows. Hence, as ' $g$ ' decrease, capacitances increase (inverse proportion), causing the resonant frequency to decrease and thus the notched bandwidth to decrease (5).

Figure 5(c) depicts the variation in VSWR between center-located ' $vias$ ' (dashed line) and offset ' $vias$ ' (solid line). An offset ' $vias$ ' means a ' $vias$ ' shifted away from the center to the edge of the EBG patch. The notched band shifted towards the lower frequency side with strong, steep, and sharp rejection when the location of the ' $vias$ ' was moved from the center to the edge. Hence, an edge-located ' $vias$ ' achieve better coupling (mismatch) than a center-located ' $vias$ '. Based on the LC model, this could be explained as the addition of inductance to the transmission line, which results in high impedance (6), and consequently a better coupling.



**Figure 4:** Surface current distributions at (a) 6GHz, (b) 9GHz, (c) 12GHz



**Figure 5:** VSWR variation (a) with different EBG patch widths ' $W_e$ ', (b) with different gap widths ' $g$ ', (c) between center-located and offset '*vias*'

#### 4.0 CONCLUSION

In this paper, wideband and dual-band antennas with band-notched characteristics realized using an EBG structure are demonstrated. Initially, a wideband antenna was designed, and then two EBGs were integrated into the wideband antenna. The wideband antenna achieved a bandwidth of 9GHz covering 5-14GHz with  $S_{11} < -10$ dB, a maximum gain of 6.8dBi, and  $VSWR < 2$  within the operational bandwidth. The EBG provided a band-notch of bandwidth 3GHz from 8-11GHz with  $S_{11} > -10$ dB, then dual-band of bandwidth 2GHz and 1.5GHz with  $S_{11} < -10$ dB centered at 7GHz and 11.45GHz, respectively. The simulation and experimental  $S_{11}$  are in good agreement. To better understand the behavior of EBG structure, surface current distribution and parametric studies were performed. The EBG provided the required band-notch by degrading the antenna matching impedance and changing the current distribution. We observe that the radiation pattern of

the antenna with EBG and the antenna without EBG gives the same pattern at the far-field. With dual 5G bands, the antenna could be a good candidate for 5G mobile wireless communication and filter applications.

#### REFERENCES

- [1] Balanis, C. A. "Antenna Theory: Analysis and Design", Third edit. John Wiley & sons, 2010.
- [2] Orakwue, S. I., and Ngah, R. "Two dimensional switched beam antenna based on cascaded butler matrix beamforming network", Niger. J. Technol., vol. 38, no. 4, 2019, pp. 1003–1009.
- [3] Jabire, A., Abdu, A., and Salisu, S. "Multiband Millimeter Wave T-Shaped Antenna With Optimized Patch Parameter Using Particle Swarm Optimization," Niger. J. Technol., vol. 36, no. 3, 2017, pp. 904–909.
- [4] Ashraf, N., Haraz, O., Ashraf, M, A., and

- Alshebeili, S. "28/38-GHz dual-band millimeter wave SIW array antenna with EBG structures for 5G applications", 2015 Int. Conf. Inf. Commun. Technol. Res., 2015, pp. 5–8.
- [5] Etor, D., Gafai, N. B., Akintunde, I. A., Awodiji, O. O., and Dodd, L. E. "Improving power transfer in rectenna via impedance matching at GHz frequencies", *Niger. J. Technol.*, vol. 40, no. 6, 2022, pp. 1072–1078.
- [6] Bello, H., and Nasidi, I. "Design and analysis of 2.4 GHz rectenna for charging low-power devices. 1", *Int. J. Inf. Process. Commun.*, vol. 7, no. 2, 2019, pp. 266–279.
- [7] Debatosh, G., and Yahia, M. M. A. "Microstrip and Printed Antennas: New Trends, Techniques and Applications", First edit. John Wiley & sons ltd, 2011.
- [8] Ofcom, "Spectrum above 6 GHz for future mobile communications," 2015.
- [9] Chen, Z. N., and Chia, M. Y. W. "Broadband Planar Antennas: Design and Applications", John Wiley & sons ltd, 2006.
- [10] Kang, L., Li, H., Wang, X., and Shi, X. "Compact Offset Microstrip-Fed MIMO Antenna for Band-Notched UWB Applications", *IEEE Antennas Wirel. Propag. Lett.*, vol. 14, no. c, 2015, pp. 1754–1757.
- [11] Kumar, A, et al. "Design of a novel compact planar monopole UWB antenna with triple band-notched characteristics", in 2nd International Conference on Signal Processing and Integrated Networks, SPIN 2015, 2015, pp. 56–59.
- [12] Gholami, F. A. R., and Zakeri, S. B. B. "Design and Analysis of a New Compact Band- Rejected UWB Antenna," in Telecommunications forum TELFOR 2012, 2012, no. 20th, pp. 1165–1167.
- [13] Fan Yang and Yahya Rahmat-Samii. "Electromagnetic Band Gap Structures in Antenna Engineering", First edit. Cambridge University Press, 2009.
- [14] Ahmad A. G., and Dimitris E. A. "Dual Band-Reject UWB Antenna With Sharp Rejection of Narrow and Closely-Spaced Bands", *IEEE Trans. Antennas Propag.*, vol. 60, no. 4, 2012, pp. 2071–2076.
- [15] Ayop, M. A. O., Rahim, M. K. A., Kamarudin, M. R., and Abdul Aziz, M. Z. A. "Dual Band Electromagnetic Band Gap Structure Incorporated with Ultra-Wideband Antenna", in Proceedings of the Fourth European Conference on Antennas and Propagation, 2010, pp. 1–4.
- [16] Yazdi, M., and Komjani, N. "Design of a band-notched UWB monopole antenna by means of an EBG structure", *IEEE Antennas Wirel. Propag. Lett.*, vol. 10, 2011, pp. 170–173.
- [17] Hirano, T., and Hirose, A. "Wideband and Low Direct-Coupling Tapered Slot Antenna Using Electromagnetic Bandgap Structures", *IEEE Trans. Antennas Propag.*, vol. 67, no. 4, 2019, pp. 2272–2279.
- [18] Siamak, E., and Abbas, S. "Mutual Coupling Reduction in Waveguide- Slot-Array Antennas Using Electromagnetic", *IEEE Antennas Propag. Mag.*, vol. 56, no. 3, 2014, pp. 68–79.
- [19] Roy, M., and Mittal, A. "Recent advancements in techniques to suppress surface wave propagation in microstrip patch antenna", 3rd IEEE Int. Conf., 2017, pp. 1–5.
- [20] Wongsan, R., Krachodnok, P., Kampeephat, S., and Kamphikul, P. "Gain enhancement for conventional circular horn antenna by using EBG technique", in 2015 12th International Conference on Electrical Engineering/ Electronics, Computer, Telecommunications and Information Technology (ECTI-CON), 2015, pp. 1–4.
- [21] Kim, M. "A Compact EBG Structure with Wideband Power/Ground Noise Suppression Using Meander-Perforated Plane", *IEEE Trans. Electromagn. Compat.*, vol. 57, no. 3, 2015, pp. 595–598.
- [22] Tripathi, J. N., Mukherjee, J., Apte, P. R., Nagpal, R. K., Chhabra, N. K., and Malik, R. "A novel EBG structure with super-wideband suppression of simultaneous switching noise in high speed circuits", in 2013 IEEE 22nd Conference on Electrical Performance of Electronic Packaging and Systems, EPEPS 2013, 2013, pp. 243–246.
- [23] Arora, A., and Kumar, N. "To reduce mutual coupling in microstrip patch antenna arrays elements using electromagnetic band gap structures for X-band", in 2017 International Conference on Nextgen Electronic Technologies: Silicon to Software, ICNETS2 2017, 2017, pp. 228–230.
- [24] Hossein Malekpoor, S. J. "Design , analysis , and modeling of miniaturized multi-band patch arrays using mushroom-type electromagnetic band gap structures", *Int. J. RF Microw. Comput. Eng.*, vol. 28, no. 6, 2018, pp. 1–13.
- [25] Fayadh, R. A., Malek, F., and Fadhil, H. A. "Spade-Shaped Patch Antenna for Ultra Wideband Wireless Communication Systems", *Int. J. Adv. Comput. Res.*, vol. 3, no. 3, 2013, pp. 16–22.

- [26] Sun, J., and Luk, K. M. "Wideband Linearly-Polarized and Circularly-Polarized Aperture-Coupled Magneto-Electric Dipole Antennas Fed by Microstrip Line With Electromagnetic Bandgap Surface", *IEEE Access*, vol. 7, no. c, 2019, pp. 43084–43091.
- [27] Khan, Q. U., and Bin Ihsan, M. "Higher order mode excitation for high gain microstrip patch antenna", *AEU - Int. J. Electron. Commun.*, vol. 68, no. 11, 2014, pp. 1073–1077.
- [28] Zhi Ning Chen, S. P. S., et al. "Printed UWB Antennas", in *Microstrip and Printed Antennas: New Trends, Techniques and Applications*, First edit., John Wiley & sons ltd, 2011, pp. 305–340.